

Green function for hyperbolic media

Andrey S. Potemkin,¹ Alexander N. Poddubny,^{1,2} Pavel A. Belov,^{1,3} and Yuri S. Kivshar,^{1,4}

¹*Department of Photonics and Optoinformatics, National University of Information Technology, Mechanics and Optics (ITMO), St. Petersburg 197101, Russia*

²*Ioffe Physical-Technical Institute of the Russian Academy of Sciences, St. Petersburg 194021, Russia*

³*School of Electronic Engineering and Computer Science,*

Queen Mary University of London, Mile End Road, London E1 4NS, UK

⁴*Nonlinear Physics Center, Research School of Physics and Engineering, Australian National University, Canberra ACT 0200, Australia*

We revisit the problem of the electromagnetic Green function for homogeneous hyperbolic media, where longitudinal and transverse components of the dielectric permittivity tensor have different signs. We analyze the dipole emission patterns for both dipole orientations with respect to the symmetry axis and for different signs of dielectric constants, and show that the emission pattern is highly anisotropic and has a characteristic cross-like shape: the waves are propagating within a certain cone and are evanescent outside this cone. We demonstrate the coexistence of the cone-like pattern due to emission of the extraordinary TM-polarized waves and elliptical pattern due to emission of ordinary TE-polarized waves. We find a singular complex term in the Green function, proportional to the δ -function and governing the photonic density of states and Purcell effect in hyperbolic media.

PACS numbers: 42.50.-p,74.25.Gz,78.70.-g

I. INTRODUCTION

Hyperbolic medium is a particular case of uniaxial anisotropic dielectric medium where the main values of the permittivity tensor $\hat{\varepsilon}$ have opposite signs [1], and the isofrequency surface of extraordinary waves is a hyperboloid. The recent attention of researchers to the hyperbolic metamaterials stems from their unique optical properties allowing negative refraction, hyperlensing and cloaking phenomena [2–4]. They are also very promising for quantum nanophotonics [5, 6], because the density of states, determined by the hyperboloid area, is divergent. This means an infinite spontaneous decay rate of a quantum emitter embedded in a hyperbolic medium, i.e. infinite Purcell effect [7]. In the realistic case, the radiation rate is limited by certain cutoffs in the wavevector space [8–11], however, experimental observation of radiative enhancement is still possible [5, 12].

A general hyperbolic medium can be characterized by a dielectric permittivity tensor

$$\hat{\varepsilon} = \begin{pmatrix} \varepsilon_{\perp} & 0 & 0 \\ 0 & \varepsilon_{\perp} & 0 \\ 0 & 0 & \varepsilon_{\parallel} \end{pmatrix}, \quad \text{Re } \varepsilon_{\perp} \text{ Re } \varepsilon_{\parallel} < 0. \quad (1)$$

Resulting isofrequency surface of extraordinary waves is a hyperboloid,

$$\frac{q_x^2 + q_y^2}{\varepsilon_{\parallel}} + \frac{q_z^2}{\varepsilon_{\perp}} = \left(\frac{\omega}{c}\right)^2. \quad (2)$$

Two different types of hyperboloids are possible for $\varepsilon_{\parallel} < 0$, $\varepsilon_{\perp} > 0$ (see Fig. 1a) and for $\varepsilon_{\parallel} > 0$, $\varepsilon_{\perp} < 0$ (see Fig. 1b).

Hyperbolic medium can be realized in several ways. First realization has been reported for magnetized

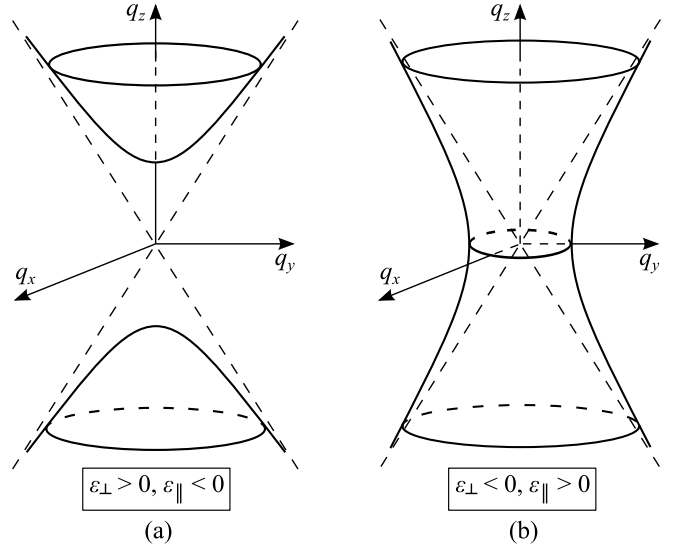


FIG. 1: Schematic illustration of the isofrequency surfaces in the wavevectors space for the hyperbolic medium with $\varepsilon_{\parallel} < 0$, $\varepsilon_{\perp} > 0$ (a) and with $\varepsilon_{\parallel} > 0$, $\varepsilon_{\perp} < 0$ (b).

plasma in microwave spectral range [13]. Under a very strong static magnetic field applied along z axis the plasma is described by the permittivity with [13, 14]

$$\varepsilon_{\perp} = 1, \quad \varepsilon_{\parallel} = 1 - \frac{\omega_p^2}{\omega^2}.$$

Thus, the frequencies ω below the plasma frequency ω_p correspond to the hyperbolic regime with $\varepsilon_{\parallel} < 0$.

The interest to the hyperbolic medium is now revived and rapidly increases due to its successful realization using artificial photonic structures, metamaterials [5, 15–18]. In particular, the layered structure composed of al-

ternating dielectric and metallic slabs is described by effective permittivities

$$\varepsilon_{\perp} = \frac{\varepsilon_1 d_1 + \varepsilon_2 d_2}{d_1 + d_2}, \quad \varepsilon_{\parallel} = \left(\frac{\varepsilon_1^{-1} d_1 + \varepsilon_2^{-1} d_2}{d_1 + d_2} \right)^{-1},$$

where $\varepsilon_1, \varepsilon_2, d_1, d_2$ are dielectric constants and thicknesses of slabs, respectively. Since dielectric constants of the metals in optical frequency range are negative, it is possible to adjust thicknesses of slabs in order to obtain either $\varepsilon_{\perp} < 0$ or $\varepsilon_{\parallel} < 0$ [19, 20]. Realizations of hyperbolic regime have been also reported for metamaterials based on nanorod arrays [16, 21, 22] and for graphite [23].

The ongoing studies of hyperbolic medium raise the demand for the general theoretical formalism. The most rigorous description of the optical properties of arbitrary photonic structure is provided by its tensor Green function [24], determined from

$$(\nabla \times \nabla \times \hat{I} - k^2 \hat{\varepsilon}) \hat{G}(\mathbf{r}) = 4\pi k^2 \hat{I} \delta(\mathbf{r}), \quad (3)$$

where \hat{I} is the unit tensor and $k = \omega/c$. Green function for medium with uniaxial permittivity tensor is presented in a number of works [1, 25–33]. Most general form of the result is given by Chen in Ref. [26] in dyadic form and by Savchenko in Ref. [32] in Cartesian form. However, despite the impressive amount of the researchers done, we are not aware of any comprehensive study of the Green function in hyperbolic case. Moreover, all existing works except [29, 31] neglect the singular term in the Green function, which, as will be shown below, is crucial for the description of the photonic density of states and Purcell enhancement in hyperbolic regime. Here we present a general theory of the Green function and dipole emission in hyperbolic medium. We analyze both types of hyperbolic medium, illustrated on Fig. 1, and both axial and transverse dipole orientations.

The rest of the paper is organized as follows. Sec. II outlines the Green function calculation. Singular term in the Green function is discussed in Sec. III. Sec. IV presents the calculated emission patterns of point dipole. Main paper results are summarized in Sec. V. Auxiliary expressions are presented in Appendices.

II. GREEN FUNCTION CALCULATION

Green function (3) may be calculated either in real space via the methods of operators [30] or in wavevector space via Fourier analysis [26]. The Fourier representation of $\hat{G}(\mathbf{r})$, defined from

$$\hat{G}(\mathbf{r}) = \int \frac{d^3 q}{(2\pi)^3} e^{i\mathbf{q}\mathbf{r}} \hat{G}(\mathbf{q}), \quad (4)$$

is given by

$$\hat{G}(\mathbf{q}) = 4\pi k^2 \left\{ \left(\varepsilon_{\perp} \varepsilon_{\parallel} \hat{\varepsilon} - \frac{\mathbf{q} \otimes \mathbf{q}}{k^2} \right) \frac{1}{q_{\parallel}^2 \varepsilon_{\parallel} + q_{\perp}^2 \varepsilon_{\perp} - k^2 \varepsilon_{\perp} \varepsilon_{\parallel}} + \frac{(\mathbf{q} \times \hat{\mathbf{z}}) \otimes (\mathbf{q} \times \hat{\mathbf{z}})}{q_{\perp}^2} \left(\frac{1}{q^2 - k^2 \varepsilon_{\perp}} - \frac{\varepsilon_{\parallel}}{q_{\parallel}^2 \varepsilon_{\parallel} + q_{\perp}^2 \varepsilon_{\perp} - k^2 \varepsilon_{\perp} \varepsilon_{\parallel}} \right) \right\}. \quad (5)$$

Here $q_{\parallel} \equiv q_z$ and $q_{\perp}^2 = q_x^2 + q_y^2$. The symbol \otimes denotes the direct product, $[\mathbf{a} \otimes \mathbf{b}]_{\alpha\beta} \equiv a_{\alpha} b_{\beta}$. The poles in Eq. (5) determine the dispersion equations of the electromagnetic waves. Two poles correspond to extraordinary (TM) waves, with magnetic field \mathbf{H} perpendicular to z axis, and to ordinary (TE) waves, with $\mathbf{E} \cdot \hat{\mathbf{z}} = 0$ and $q = k\sqrt{\varepsilon_{\perp}}$.

Both direct and reciprocal space methods give the same following result for the Green function:

$$\hat{G}(\mathbf{r}) = \frac{1}{\sqrt{\varepsilon_{\perp}}} \left\{ (k^2 \hat{\varepsilon} + \nabla \otimes \nabla) \frac{e^{ikr_e}}{r_e} + k^2 \left(\varepsilon_{\perp} \frac{e^{ikr_o}}{r_o} - \varepsilon_{\parallel} \frac{e^{ikr_e}}{r_e} \right) \frac{(\mathbf{r} \times \hat{\mathbf{z}}) \otimes (\mathbf{r} \times \hat{\mathbf{z}})}{(\mathbf{r} \times \hat{\mathbf{z}})^2} - ik \frac{e^{ikr_o} - e^{ikr_e}}{(\mathbf{r} \times \hat{\mathbf{z}})^2} \left(\hat{\mathbf{I}} - \hat{\mathbf{z}} \otimes \hat{\mathbf{z}} - \frac{2(\mathbf{r} \times \hat{\mathbf{z}}) \otimes (\mathbf{r} \times \hat{\mathbf{z}})}{(\mathbf{r} \times \hat{\mathbf{z}})^2} \right) \right\}, \quad (6)$$

where

$$\hat{\varepsilon} \equiv \varepsilon_{\perp} \varepsilon_{\parallel} \hat{\varepsilon}^{-1} = \varepsilon_{\parallel} (\hat{\mathbf{I}} - \hat{\mathbf{z}} \otimes \hat{\mathbf{z}}) + \varepsilon_{\perp} \hat{\mathbf{z}} \otimes \hat{\mathbf{z}},$$

$$r_e = \sqrt{\mathbf{r}(\hat{\varepsilon}\mathbf{r})} = \sqrt{\varepsilon_{\parallel}(x^2 + y^2) + \varepsilon_{\perp} z^2}, \quad r_o = \sqrt{\varepsilon_{\perp}} r.$$

This result was obtained without any assumptions for signs of real of parts ε_{\perp} and ε_{\parallel} and is applicable to case of hyperbolic medium. Imaginary parts of ε_{\perp} and ε_{\parallel} and of the square roots in expressions for r_e and r_o should be positive (we assume the time dependence $e^{-i\omega t}$).

Eq. (6) is not the final result for the Green function yet, because the derivative in the term $\nabla \otimes \nabla e^{ikr_e}/r_e$ is not evaluated. Some authors [30, 33] leave the expression for $\hat{G}(\mathbf{r})$ in the form (6) without taking this derivatives. However, this term produces singularity in $\hat{G}(\mathbf{r})$. The nature of this singularity is the same for the well-known identity

$$\Delta \frac{1}{r} = -4\pi \delta(\mathbf{r}).$$

Calculating the derivative we obtain the final expres-

sion of singular Green function:

$$\begin{aligned} \hat{G}(\mathbf{r}) = & \hat{G}_{\text{sing}}(\mathbf{r}) + \frac{1}{\sqrt{\varepsilon_{\perp}}} \left\{ k^2 \frac{e^{ikr_e}}{r_e} \left(1 - \frac{1}{ikr_e} - \frac{1}{k^2 r_e^2} \right) \hat{\varepsilon} \right. \\ & - k^2 \frac{e^{ikr_e}}{r_e^3} \left(1 - \frac{3}{ikr_e} - \frac{3}{r_e^2} \right) (\hat{\varepsilon}\mathbf{r}) \otimes (\hat{\varepsilon}\mathbf{r}) \\ & + k^2 \left(\varepsilon_{\perp} \frac{e^{ikr_o}}{r_o} - \varepsilon_{\parallel} \frac{e^{ikr_e}}{r_e} \right) \frac{(\mathbf{r} \times \hat{\mathbf{z}}) \otimes (\mathbf{r} \times \hat{\mathbf{z}})}{(\mathbf{r} \times \hat{\mathbf{z}})^2} \\ & \left. - ik \frac{e^{ikr_o} - e^{ikr_e}}{(\mathbf{r} \times \hat{\mathbf{z}})^2} \left(\hat{\mathbf{1}} - \hat{\mathbf{z}} \otimes \hat{\mathbf{z}} - \frac{2(\mathbf{r} \times \hat{\mathbf{z}}) \otimes (\mathbf{r} \times \hat{\mathbf{z}})}{(\mathbf{r} \times \hat{\mathbf{z}})^2} \right) \right\}, \end{aligned} \quad (7)$$

where $\hat{G}_{\text{sing}}(\mathbf{r})$ stands for the singular contribution

$$\begin{aligned} \hat{G}_{\text{sing}}(\mathbf{r}) = & \left[(\nabla \otimes \nabla) \frac{1}{\sqrt{\varepsilon_{\perp} r_e}} \right]_{\text{sing}} \\ \equiv & -4\pi \int \frac{d^3 q}{(2\pi)^3} e^{i\mathbf{q}\mathbf{r}} \frac{\mathbf{q} \otimes \mathbf{q}}{q_{\parallel}^2 \varepsilon_{\parallel} + q_{\perp}^2 \varepsilon_{\perp}}. \end{aligned} \quad (8)$$

In general case we failed to obtain a closed answer for \hat{G}_{sing} via ordinary functions and δ -function. Eq. (8) should be understood instead only as generalized function, i.e., only its convolutions with ordinary test functions are relevant [34]. Singular Green function is essential in the hyperbolic case since it solely accounts for the diverging Purcell factor. Eqs. (7),(8) are the central result of this work. It is valid for both hyperbolic and elliptic media with arbitrary signs of real parts of dielectric constants.

III. SINGULAR TERM OF GREEN FUNCTION

Singular term in the Green function should be treated with extra care [35–37]. Functional (8) may be explicitly written out in only isotropic medium with $\varepsilon_{\parallel} = \varepsilon_{\perp} \equiv \varepsilon$ [38]:

$$\hat{G}_{\text{sing}}(\mathbf{r}) = -\frac{4\pi}{\varepsilon} \frac{\mathbf{r} \otimes \mathbf{r}}{r^2} \delta(\mathbf{r}). \quad (9)$$

In general anisotropic case we have not found a closed form answer. Previous expression for this functional in anisotropic medium, obtain by Weiglhofer [28, 29],

$$-\frac{4\pi}{3} \hat{\varepsilon}^{-1} \delta(\mathbf{r}) \quad (10)$$

is obviously wrong since it has been obtained as a naive generalization of the result [39]

$$-\frac{4\pi}{3\varepsilon} \delta(\mathbf{r}) \quad (11)$$

for the isotropic medium. Despite the fact that functional (11) is frequently used [39], it gives different results than Eq. (9) when applied to functions, non-analytical in the point $\mathbf{r} = 0$, such as $\mathbf{r} \otimes \mathbf{r}/r^2$. This discrepancy is

discussed in Ref. [38] in details. Since angular averaging of $\mathbf{r} \otimes \mathbf{r}$ equals to $1/3$, both functionals (11) and (9) may give the same result for some test functions. However, straightforward generalization of Eq. (11) to Eq. (10) is not valid since not all rules of normal calculus may be applied to generalized functions [34].

Explicit form of the functional (8) in anisotropic case can be obtained within the space of the test functions, analytical in the point $\mathbf{r} = 0$:

$$\begin{aligned} \hat{G}_{\text{sing}}(\mathbf{r}) = & \frac{2\pi\delta(\mathbf{r})}{\varepsilon_{\parallel} - \varepsilon_{\perp}} \left[\hat{\mathbf{x}} \otimes \hat{\mathbf{x}} + \hat{\mathbf{y}} \otimes \hat{\mathbf{y}} - 2\hat{\mathbf{z}} \otimes \hat{\mathbf{z}} \right. \\ & + \arctan(\sqrt{\varepsilon_{\parallel}/\varepsilon_{\perp} - 1}) \left(\frac{2}{\sqrt{\varepsilon_{\parallel}/\varepsilon_{\perp} - 1}} \hat{\mathbf{z}} \otimes \hat{\mathbf{z}} \right. \\ & \left. \left. - \frac{\varepsilon_{\parallel}}{\varepsilon_{\perp} \sqrt{\varepsilon_{\parallel}/\varepsilon_{\perp} - 1}} (\hat{\mathbf{x}} \otimes \hat{\mathbf{x}} + \hat{\mathbf{y}} \otimes \hat{\mathbf{y}}) \right) \right]. \end{aligned} \quad (12)$$

The equivalence between Eq. (12) and Eq. (8) for test functions, analytical in the point $r = 0$ is directly shown via real space integration in spherical coordinates. Let us demonstrate it for zz component:

$$\begin{aligned} \int_{r < R} d^3 r [G_{\text{sing}}]_{zz}(\mathbf{r}) &= \int_{r < R} d^3 r \frac{\partial^2}{\partial z^2} \frac{1}{\sqrt{\varepsilon_{\perp} r_e}} \\ &= \oint_{r=R} d\mathbf{S} \cdot \hat{\mathbf{z}} \frac{\partial}{\partial z} \frac{1}{\sqrt{\varepsilon_{\perp} r_e}} \\ &= -2\pi \sqrt{\varepsilon_{\perp}} \int_0^{\pi} d\theta \frac{\sin \theta \cos^2 \theta}{(\varepsilon_{\parallel} \sin^2 \theta + \varepsilon_{\perp} \cos^2 \theta)^{3/2}}. \end{aligned} \quad (13)$$

Performing the integral over θ we obtain expression, equal to $\int d^3 r [\hat{G}_{\text{sing}}]_{zz}(\mathbf{r})$ which finalizes the proof. Eq. (12) also follows from the wavevector-space representation in Eq. (8). In the limit $\varepsilon_{\perp} = \varepsilon_{\parallel}$ Eq. (12) reduces to Eq. (11). Obviously, functional (12) is far more complex than (wrong) Eq. (10). Still, it is valid for narrower set of test functions than Eqs. (8),(9).

One may think that this singular terms are of purely mathematical interest. Counterintuitively, they may control such observable quantities, as photonic density of states and Purcell factor. In particular, in the case of lossless hyperbolic medium ($\varepsilon_{\parallel} \varepsilon_{\perp} < 0$, $\text{Im} \varepsilon_{\parallel}, \varepsilon_{\perp} \rightarrow +0$) the singular part of the Green function acquires non-zero imaginary part,

$$\begin{aligned} \text{Im} \hat{G}_{\text{sing}}(\mathbf{r}) = & \frac{2\pi^2 \sqrt{|\varepsilon_{\perp}|}}{(|\varepsilon_{\perp}| + |\varepsilon_{\parallel}|)^{3/2}} \delta(\mathbf{r}) \\ & \times \left[\hat{\mathbf{z}} \otimes \hat{\mathbf{z}} + \frac{|\varepsilon_{\parallel}|}{|\varepsilon_{\perp}|} (\hat{\mathbf{x}} \otimes \hat{\mathbf{x}} + \hat{\mathbf{y}} \otimes \hat{\mathbf{y}}) \right]. \end{aligned} \quad (14)$$

The singularity in Eq. (14) is a direct consequence of the infinite density of TM modes Eq. (2). Green function where this singularity is omitted has wrong analytical properties and can not be used for nanophotonic applications

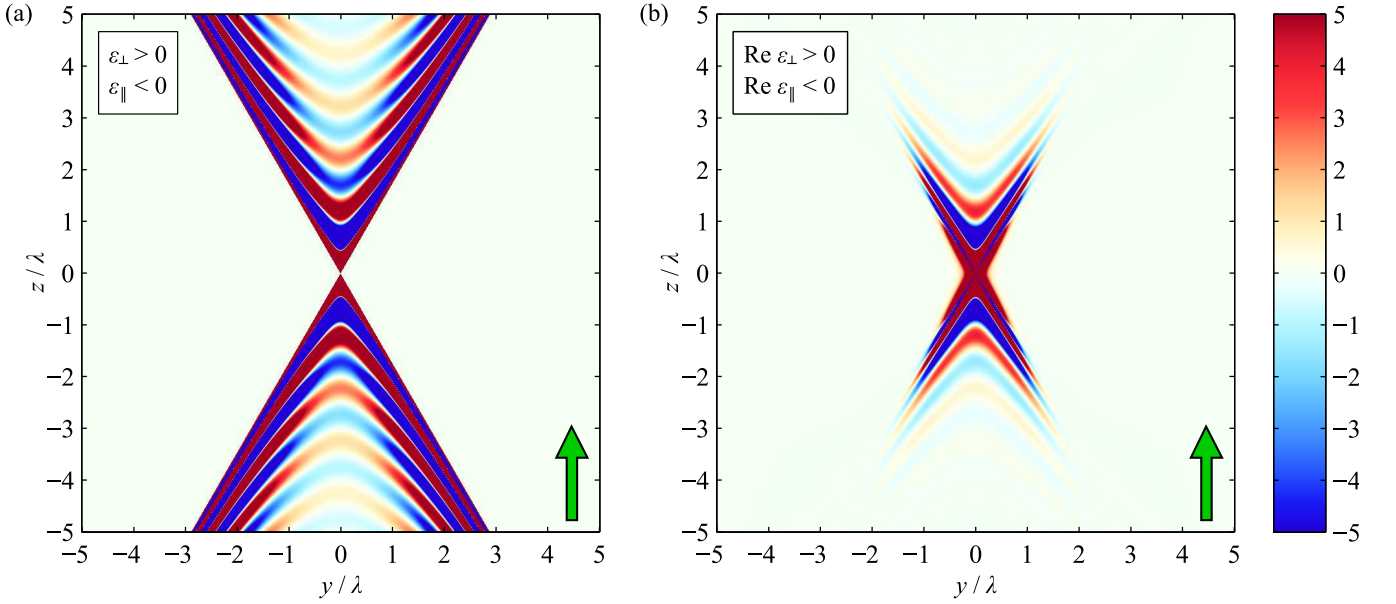


FIG. 2: Dipole field $\lambda^3 E_z(0, y, z)$ in hyperbolic medium with $\varepsilon_{\perp} = 1$, $\varepsilon_{\parallel} = -3$ (a) and with $\varepsilon_{\perp} = 1 + 0.2i$, $\varepsilon_{\parallel} = -3 + 0.2i$ (with losses) (b). Dipole moment is parallel to the axis of anisotropy $\hat{\mathbf{z}}$.

such as Purcell factor calculation. Generally, the Purcell factor of the embedded light emitter oriented along $\hat{\mathbf{n}}$ direction can be found[40] as

$$f = \frac{3}{2k^3} \text{Im} \hat{\mathbf{n}} \cdot \hat{G}(0) \hat{\mathbf{n}}. \quad (15)$$

Due to the singularity in the local density of states Eq. (15) provides diverging Purcell factor. As has been indicated in our previous work [8], this divergence is smeared out for finite size emitter, characterized with spatial distribution $\Phi(\mathbf{r})$, normalized as $\int d^3r \Phi(\mathbf{r}) = 1$. In case of the semiconductor quantum dot $\Phi(\mathbf{r})$ is proportional to the exciton envelope function [41]. For distributed source Eq. (15) is replaced by

$$f = \frac{3}{2k^3} \hat{\mathbf{n}} \cdot \int d^3r d^3r' \Phi(\mathbf{r}) \Phi(\mathbf{r}') \hat{G}(\mathbf{r} - \mathbf{r}') \hat{\mathbf{n}}. \quad (16)$$

In the case of isotropic source distribution, $\Phi(\mathbf{r}) \equiv \Phi(r)$, the Purcell factor is readily evaluated using (14) and is proportional to the cube of the ratio of the wavelength and the size of the source.

IV. DIPOLE EMISSION PATTERN

Green function (3) allows to find electric field for arbitrary distribution of polarization $\mathbf{P}(\mathbf{r})$,

$$\mathbf{E}(\mathbf{r}) = \int d^3r' \hat{G}(\mathbf{r} - \mathbf{r}') \mathbf{P}(\mathbf{r}'). \quad (17)$$

For the point dipole \mathbf{p} one has $\mathbf{P}(\mathbf{r}) = \mathbf{p} \delta(\mathbf{r})$ and the electric field is given by

$$\mathbf{E}(\mathbf{r}) = \hat{G}(\mathbf{r}) \cdot \mathbf{p}. \quad (18)$$

In the following subsections we consider two principal cases of orientation of dipole moment \mathbf{p} with respect to the anisotropy axis $\hat{\mathbf{z}}$.

It should be noted that the regular part of the dipole field may be easily obtained without knowledge of the dyadic Green function (7). Electromagnetic field in the uniaxial medium can be decomposed into two parts: TM-field, where $\mathbf{H} \cdot \hat{\mathbf{z}}$ is zero, and TE-field, where $\mathbf{E} \cdot \hat{\mathbf{z}}$ is zero [25]. Solutions for these fields in hyperbolic medium can be found separately via corresponding solutions in vacuum using of anisotropic scaling method introduced by Clemmow in Ref. [42]. The key point of this method consists in appropriate scaling of space as well as fields and polarizations from Maxwell's equations in vacuum to obtain expressions for fields and currents in anisotropic medium. Application of Clemmow's method for hyperbolic medium gives the following scaling rules:

(i) TE polarization

$$\mathbf{E}(\mathbf{r}) = \hat{\varepsilon}^{1/2} \mathbf{E}_0(\hat{\varepsilon}^{1/2} \mathbf{r}), \quad (19)$$

$$\mathbf{H}(\mathbf{r}) = \sqrt{\varepsilon_{\perp} \varepsilon_{\parallel}} \mathbf{H}_0(\hat{\varepsilon}^{1/2} \mathbf{r}), \quad (20)$$

$$\mathbf{P}(\mathbf{r}) = \sqrt{\varepsilon_{\perp} \varepsilon_{\parallel}} \hat{\varepsilon}^{1/2} \mathbf{P}_0(\hat{\varepsilon}^{1/2} \mathbf{r}), \quad (21)$$

(ii) TM polarization

$$\mathbf{E}(\mathbf{r}) = \mathbf{E}_0(\sqrt{\varepsilon_{\perp}} \mathbf{r}), \quad (22)$$

$$\mathbf{H}(\mathbf{r}) = \sqrt{\varepsilon_{\perp}} \mathbf{H}_0(\sqrt{\varepsilon_{\perp}} \mathbf{r}), \quad (23)$$

$$\mathbf{P}(\mathbf{r}) = \varepsilon_{\perp} \mathbf{P}_0(\sqrt{\varepsilon_{\perp}} \mathbf{r}), \quad (24)$$

where $\mathbf{E}_0, \mathbf{H}_0, \mathbf{P}_0$ are vacuum solutions and

$$\hat{\varepsilon}^{1/2} = \sqrt{\varepsilon_{\perp}} (\hat{\mathbf{I}} - \hat{\mathbf{z}} \otimes \hat{\mathbf{z}}) + \sqrt{\varepsilon_{\parallel}} \hat{\mathbf{z}} \otimes \hat{\mathbf{z}},$$

$$\hat{\varepsilon}^{1/2} = \sqrt{\varepsilon_{\parallel}} (\hat{\mathbf{I}} - \hat{\mathbf{z}} \otimes \hat{\mathbf{z}}) + \sqrt{\varepsilon_{\perp}} \hat{\mathbf{z}} \otimes \hat{\mathbf{z}}.$$

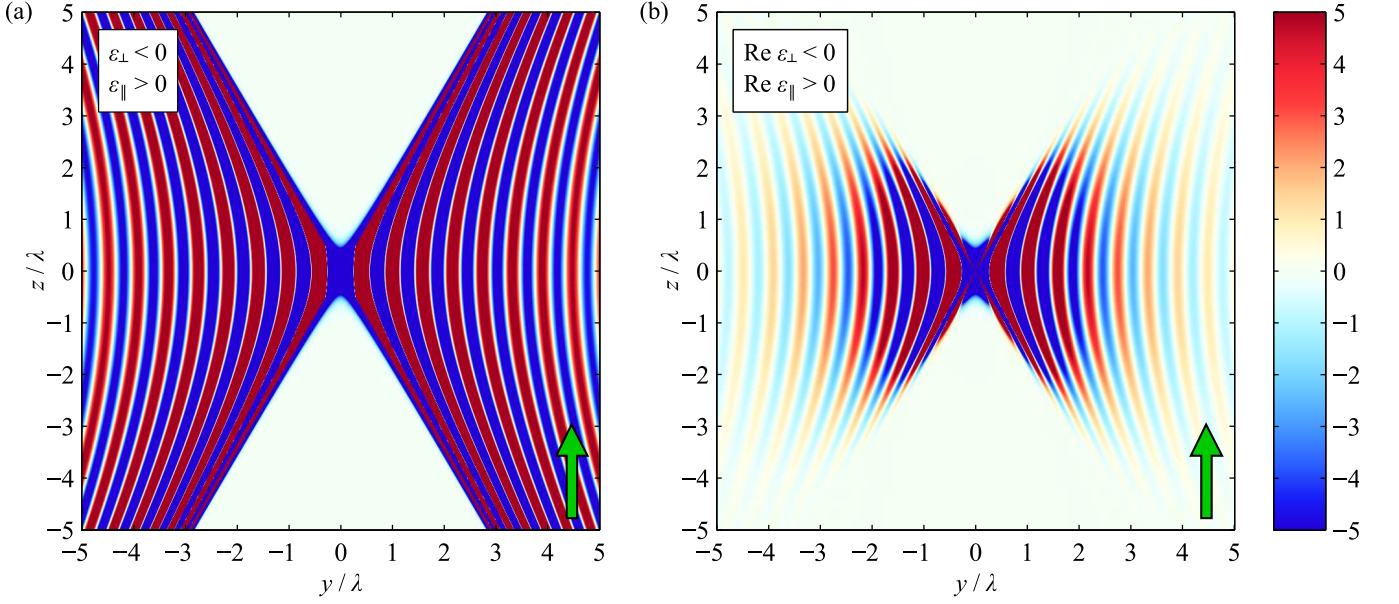


FIG. 3: Dipole field $\lambda^3 E_z(0, y, z)$ in hyperbolic medium with $\varepsilon_{\perp} = -1$, $\varepsilon_{\parallel} = 3$ (a) and with $\varepsilon_{\perp} = -1 + 0.2i$, $\varepsilon_{\parallel} = 3 + 0.2i$ (with losses) (b). Dipole moment is parallel to the axis of anisotropy $\hat{\mathbf{z}}$.

Decomposition of the dipole polarization \mathbf{P} into the TM/TE parts is described in [43, 44].

A. Dipole parallel to the axis of anisotropy

Here we consider the case $\mathbf{p} = p\hat{\mathbf{z}}$. Taking into account that

$$\begin{aligned} \hat{\varepsilon} \cdot \hat{\mathbf{z}} &= \varepsilon_{\perp} \hat{\mathbf{z}}, & (\hat{\varepsilon} \mathbf{r}) \cdot \hat{\mathbf{z}} &= \varepsilon_{\perp} \mathbf{r} \cdot \hat{\mathbf{z}}, \\ (\mathbf{r} \times \hat{\mathbf{z}}) \cdot \hat{\mathbf{z}} &= 0, & (\hat{\mathbf{I}} - \hat{\mathbf{z}} \otimes \hat{\mathbf{z}}) \cdot \hat{\mathbf{z}} &= 0, \end{aligned}$$

we obtain from Eqs. (7), (18) the following result for the regular part of the electric field:

$$\begin{aligned} [\mathbf{E}(\mathbf{r})]_{\text{reg}} &= pk^2 \sqrt{\varepsilon_{\perp}} \frac{e^{ikr_e}}{r_e} \left(1 - \frac{1}{ikr_e} - \frac{1}{k^2 r_e^2} \right) \hat{\mathbf{z}} \\ &\quad - pk^2 \sqrt{\varepsilon_{\perp}} \frac{e^{ikr_e}}{r_e^3} \left(1 - \frac{3}{ikr_e} - \frac{3}{k^2 r_e^2} \right) (\mathbf{r} \cdot \hat{\mathbf{z}}) (\hat{\varepsilon} \mathbf{r}) \end{aligned} \quad (25)$$

Cartesian representation of this expression is presented in A. We see that the axial dipole emits only TM-polarized (extraordinary) waves. Calculated cross-section of the electric field in the yz plane is presented in Fig. 2, Fig. 3 for two both cases of hyperbolic medium, illustrated in Fig. 1: $\text{Re} \varepsilon_{\parallel} < 0, \text{Re} \varepsilon_{\perp} > 0$ and $\text{Re} \varepsilon_{\parallel} > 0, \text{Re} \varepsilon_{\perp} < 0$, respectively. Electric field pattern has a distinct cone-like shape: the waves are emitted only within the polar angles θ , satisfying $\varepsilon_{\parallel} \sin^2 \theta + \varepsilon_{\perp} \cos^2 \theta > 0$. This radiation pattern, characteristic for hyperbolic medium, survives even when the losses are introduced, see Fig. 2b and Fig. 3b. An interesting feature of Eq. (IV B), revealed in Fig. 2, is that $|E_z(0, 0, z)|$ is not zero for axial dipole orientation

and decays as $1/|z|$. This means that in the anisotropic medium the field is nonzero even along the direction of the dipole $\hat{\mathbf{z}}$.

B. Dipole orthogonal to the axis of anisotropy

Here we consider the case $\mathbf{p} = p\hat{\mathbf{y}}$. Taking into account that

$$\hat{\varepsilon} \cdot \hat{\mathbf{y}} = \varepsilon_{\parallel} \hat{\mathbf{y}}, \quad (\hat{\varepsilon} \mathbf{r}) \cdot \hat{\mathbf{y}} = \varepsilon_{\parallel} \mathbf{r} \cdot \hat{\mathbf{y}},$$

we obtain from (7), (18) the following result:

$$\begin{aligned} [\mathbf{E}(\mathbf{r})]_{\text{reg}} &= pk^2 \frac{\varepsilon_{\parallel}}{\sqrt{\varepsilon_{\perp}}} \frac{e^{ikr_e}}{r_e} \left(1 - \frac{1}{ikr_e} - \frac{1}{k^2 r_e^2} \right) \hat{\mathbf{y}} \\ &\quad - pk^2 \frac{\varepsilon_{\parallel}}{\sqrt{\varepsilon_{\perp}}} \frac{e^{ikr_e}}{r_e^3} \left(1 - \frac{3}{ikr_e} - \frac{3}{k^2 r_e^2} \right) (\mathbf{r} \cdot \hat{\mathbf{y}}) (\hat{\varepsilon} \mathbf{r}) \\ &\quad + pk^2 \left(\sqrt{\varepsilon_{\perp}} \frac{e^{ikr_o}}{r_o} - \frac{\varepsilon_{\parallel}}{\sqrt{\varepsilon_{\perp}}} \frac{e^{ikr_e}}{r_e} \right) \frac{[(\mathbf{r} \times \hat{\mathbf{z}}) \cdot \hat{\mathbf{y}}] (\mathbf{r} \times \hat{\mathbf{z}})}{(\mathbf{r} \times \hat{\mathbf{z}})^2} \\ &\quad - ipk \frac{1}{\sqrt{\varepsilon_{\perp}}} \frac{e^{ikr_o} - e^{ikr_e}}{(\mathbf{r} \times \hat{\mathbf{z}})^2} \left(\hat{\mathbf{y}} - \frac{2[(\mathbf{r} \times \hat{\mathbf{z}}) \cdot \hat{\mathbf{y}}] (\mathbf{r} \times \hat{\mathbf{z}})}{(\mathbf{r} \times \hat{\mathbf{z}})^2} \right). \end{aligned} \quad (26)$$

Cartesian representation of the last expression is presented in B. For this geometry both TE and TM polarized waves are emitted. Equation (26) includes the denominator $(\mathbf{r} \times \hat{\mathbf{z}})^2 \equiv x^2 + y^2$ which turns to zero at the line $x = y = 0$. However, careful analysis of Eq. (26) ensures, that electric field is continuous at this line since diverging TE and TM wave contributions cancel each other. Calculated emission pattern is presented in Figs. 4,5 for different signs of dielectric constants. Most interesting results

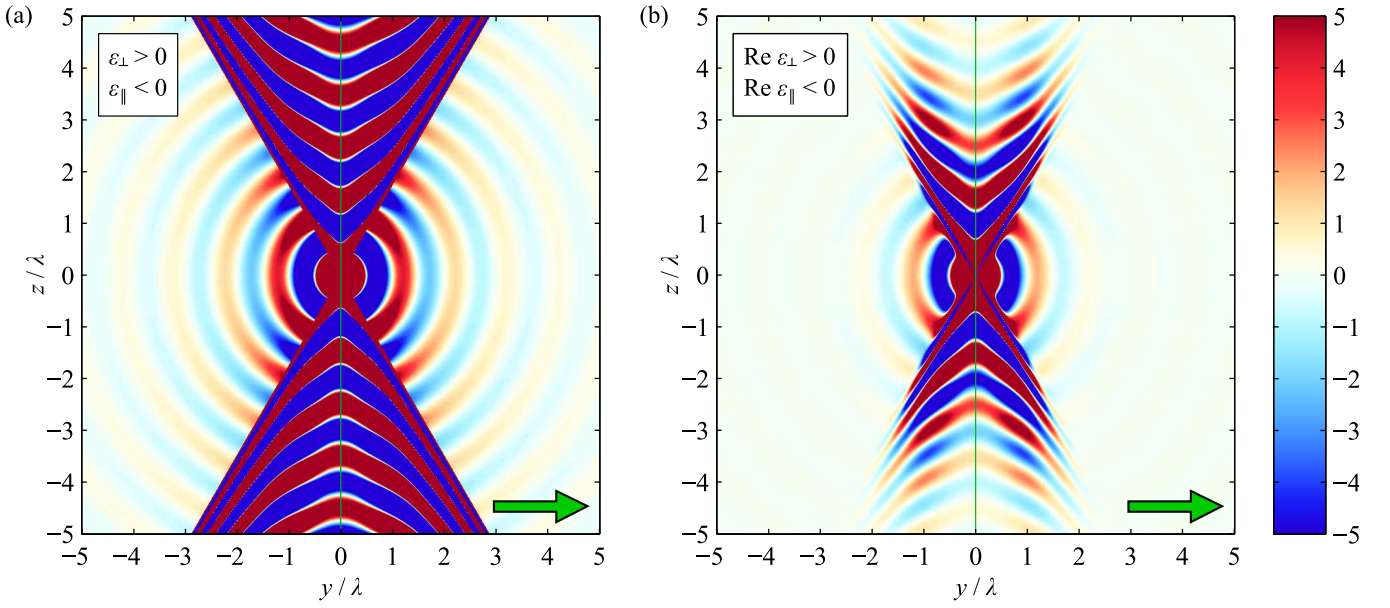


FIG. 4: Dipole field $\lambda^3 E_y(0, y, z)$ in hyperbolic medium with $\varepsilon_{\perp} = 1$, $\varepsilon_{\parallel} = -3$ (a) and with $\varepsilon_{\perp} = 1 + 0.2i$, $\varepsilon_{\parallel} = -3 + 0.2i$ (with losses) (b). Dipole moment is orthogonal to the axis of anisotropy $\hat{\mathbf{z}}$.

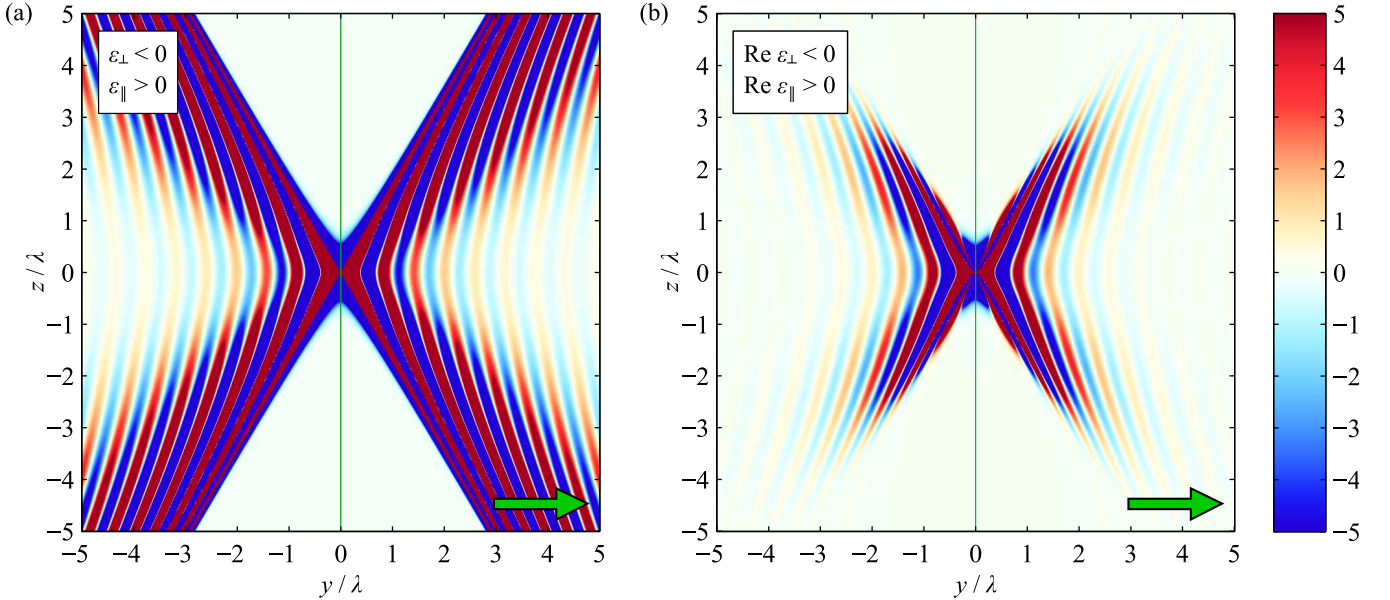


FIG. 5: Dipole field $\lambda^3 E_y(0, y, z)$ in hyperbolic medium with $\varepsilon_{\perp} = -1$, $\varepsilon_{\parallel} = 3$ (a) and with $\varepsilon_{\perp} = -1 + 0.2i$, $\varepsilon_{\parallel} = 3 + 0.2i$ (with losses) (b). Dipole moment is orthogonal to the axis of anisotropy $\hat{\mathbf{z}}$.

are manifested for $\text{Re } \varepsilon_{\parallel} < 0, \text{Re } \varepsilon_{\perp} > 0$ (Fig. 4), when the electric field is a distinct superposition of the conic pattern due to the TM waves emission and elliptic pattern due to TE waves. In the second case $\text{Re } \varepsilon_{\parallel} > 0, \text{Re } \varepsilon_{\perp} < 0$ (Fig. 5) the TE waves contribution leads just to the spatial modulation of the conic radiation pattern. Similar to the case of the axial dipole orientation, the far field is present even along the dipole direction.

Interesting results are also revealed in the Poynting vector distribution, shown in Figs. 6,7. The Poynting vector is found as $\mathbf{S} = c/(4\pi) \text{Re } \mathbf{E} \times \mathbf{H}^*$, explicit expressions for magnetic field \mathbf{H} are presented in A,B. The Poynting vector pattern inherits the conic shape from the electric field. Its largest values are achieved at the conical surface $r_e^2 = 0$. Interesting features are observed for the Poynting vector distribution in case of perpen-

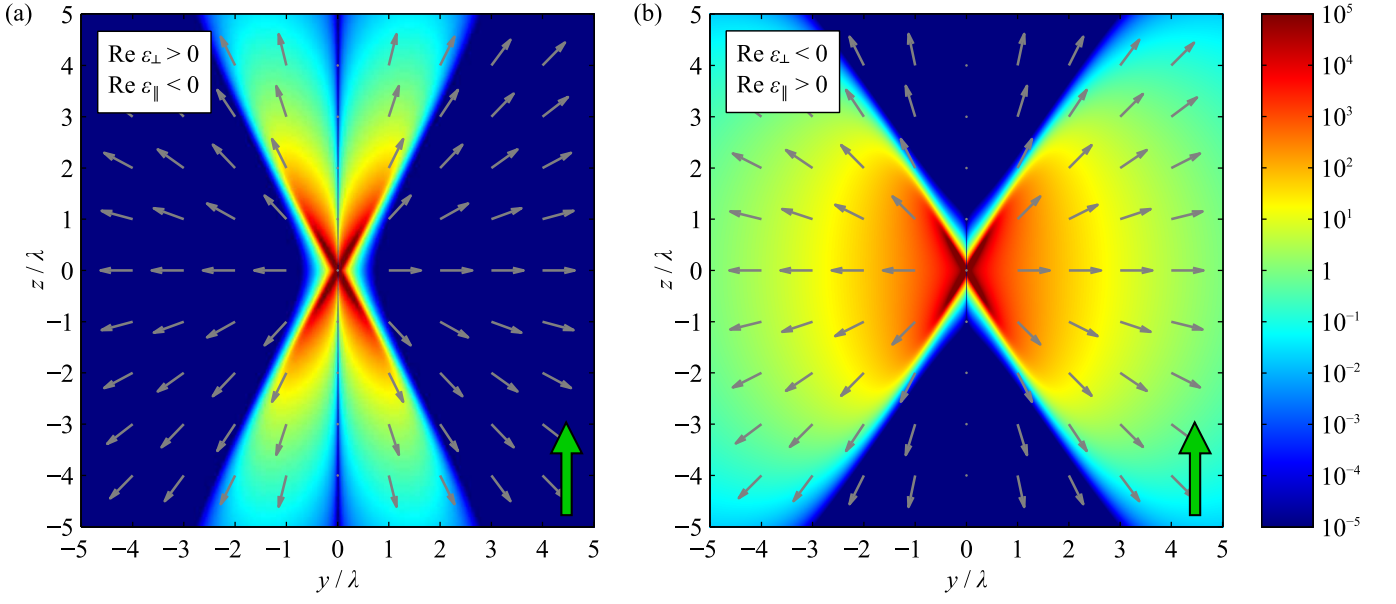


FIG. 6: Poynting vector $4\pi/(c\lambda^6)\mathbf{S}(0, y, z)$ in hyperbolic medium with $\varepsilon_{\perp} = 1+0.2i$, $\varepsilon_{\parallel} = -3+0.2i$ (a) and with $\varepsilon_{\perp} = -1+0.2i$, $\varepsilon_{\parallel} = 3+0.2i$ (b). Dipole moment is parallel to the axis of anisotropy $\hat{\mathbf{z}}$.

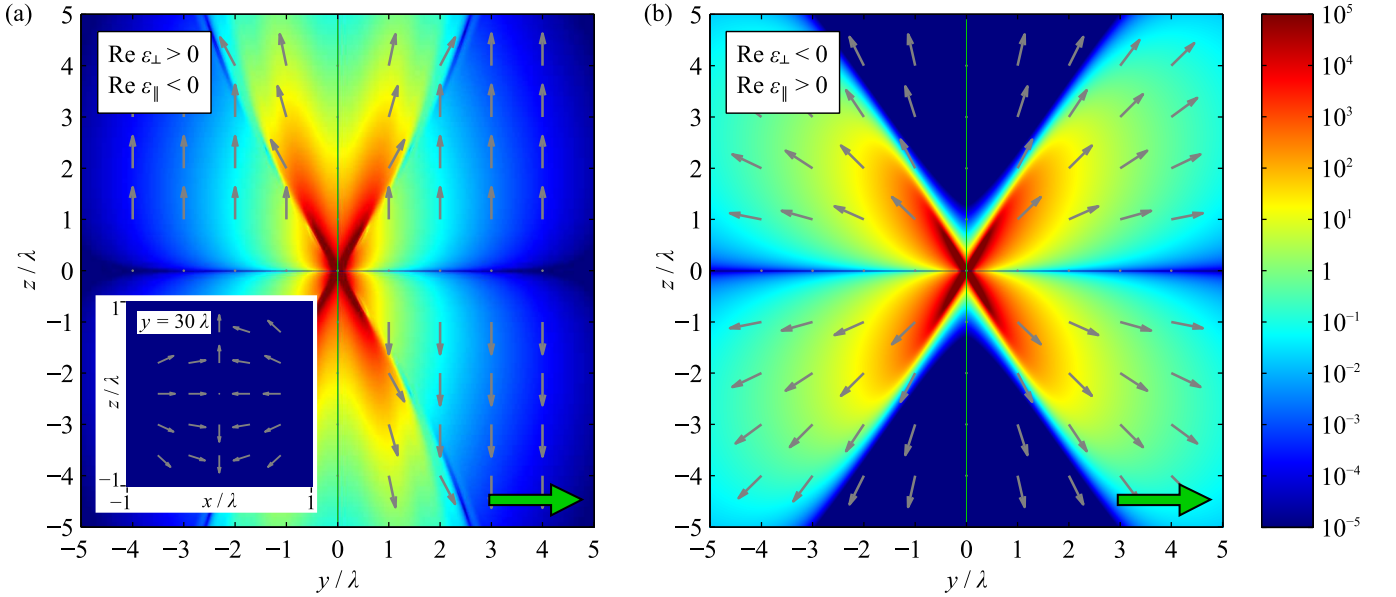


FIG. 7: Poynting vector $4\pi/(c\lambda^6)\mathbf{S}(0, y, z)$ in hyperbolic medium with $\varepsilon_{\perp} = 1+0.2i$, $\varepsilon_{\parallel} = -3+0.2i$ (a) and with $\varepsilon_{\perp} = -1+0.2i$, $\varepsilon_{\parallel} = 3+0.2i$ (b). Dipole moment is orthogonal to the axis of anisotropy $\hat{\mathbf{z}}$. Inset in panel (a) illustrates the Poynting vector distribution in the xz plane for $y = 30\lambda$.

dipole orientation and $\text{Re } \varepsilon_{\parallel} < 0$, illustrated on Fig. 7a. In the region outside of the cone, $r_e^2 < 0$, the Poynting vector in the yz plane is directed almost along the z direction. The resulting pattern looks as if there is a line source located at $y = x = 0$, which violates the energy conservation condition. However, this first impression is wrong. Close inspection of the Poynting vector distribution reveals that the line $y = x = 0$ is a saddle

point of the Poynting vector: the energy enters the line along x direction and leaves along z one. This behavior is illustrated in the xz cross-section of the Poynting vector distribution, shown in the inset of Fig. 7a.

One can also prove this result analytically. Neglecting the evanescent terms $\propto \exp(-k|r_e|)$ we find following

expression for the Poynting vector for vanishing losses

$$\mathbf{S} = \frac{c}{4\pi r^{3/2}(x^2 + y^2)^2 \sqrt{\varepsilon_{\perp}}} \quad (27)$$

$$\times \left\{ \hat{\mathbf{x}} [k^2 \varepsilon_{\perp} x^3 (x^2 + y^2) + x(x^2 - y^2)] \right.$$

$$+ \hat{\mathbf{y}} [k^2 \varepsilon_{\perp} x^2 y (x^2 + y^2) + 2x^2 y]$$

$$\left. + \hat{\mathbf{z}} [k^2 \varepsilon_{\perp} x^2 z (x^2 + y^2) + z(r^2 + y^2)] \right\}.$$

Direct differentiation of Eq. (27) demonstrates that $\nabla \cdot \mathbf{S} = 0$, i.e., energy conservation law is fulfilled. In the limit $|x|, |z| \ll y, 1/k$ we find $\mathbf{S} \propto (z\hat{\mathbf{z}} - x\hat{\mathbf{x}})/|y^4|$, which confirms existence of the saddle point in the Poynting vector pattern.

V. CONCLUSIONS

We have presented a general theory of the dipole emission in homogeneous hyperbolic media. Using both Fourier space approach and electromagnetic scaling, we have obtained a general expression for the electromagnetic Green function, and demonstrated that the emission pattern is highly anisotropic. For dipole orientation parallel to the symmetry axis, only TM-polarized waves are excited and the emission pattern has a cone-like shape with propagating waves present only within the cone $\varepsilon_{\parallel} \sin^2 \theta + \varepsilon_{\perp} \cos^2 \theta > 0$, where θ is the polar angle. In case of the perpendicular orientation, the electric field is given by a sum of TE-polarized and TM-polarized contributions, so the waves can propagate also outside the cone. We have revealed the importance of a singular term in the Green function, and have demonstrated that it is of crucial importance for calculation of the radiative rate of light source embedded in a hyperbolic medium. In the conventional case, the singular term proportional to the δ -function is usually neglected, and it does not contribute to the Purcell factor. However, in hyperbolic media this singular term is complex even for vanishing losses, and it determines the diverging radiative decay rate.

VI. ACKNOWLEDGEMENTS

This work has been supported by the Ministry of Education and Science of Russian Federation, the Dynasty Foundation, Russian Foundation for Basic Research, European project POLAPHEN, EPSRC (UK), and the Australian Research Council. The authors acknowledge useful discussions with S.I. Maslovski, I.Yu. Popov, and C.R. Simovski.

Appendix A: Cartesian representation of the field of dipole parallel to the anisotropy axis

Cartesian components of the electric field Eq. (IV B) of the dipole oriented along the anisotropy axis z read

$$E_x = -pk^2 \varepsilon_{\parallel} \sqrt{\varepsilon_{\perp}} \frac{e^{ikr_e}}{r_e^3} \left(1 - \frac{3}{ikr_e} - \frac{3}{k^2 r_e^2} \right) xz,$$

$$E_y = -pk^2 \varepsilon_{\parallel} \sqrt{\varepsilon_{\perp}} \frac{e^{ikr_e}}{r_e^3} \left(1 - \frac{3}{ikr_e} - \frac{3}{k^2 r_e^2} \right) yz, \quad (A1)$$

$$E_z = pk^2 \varepsilon_{\parallel} \sqrt{\varepsilon_{\perp}} \frac{e^{ikr_e}}{r_e^3} \times \left[x^2 + y^2 - \left(\frac{1}{ikr_e} + \frac{1}{k^2 r_e^2} \right) \left(x^2 + y^2 - \frac{2\varepsilon_{\perp}}{\varepsilon_{\parallel}} z^2 \right) \right],$$

where $r_e = \sqrt{\varepsilon_{\parallel}(x^2 + y^2) + \varepsilon_{\perp} z^2}$. Similar result has been obtained in Ref. [32]. Magnetic field can be found as $\mathbf{H} = -(i/k)\nabla \times \mathbf{E}$:

$$H_x = pk^2 \varepsilon_{\parallel} \sqrt{\varepsilon_{\perp}} \frac{e^{ikr_e}}{r_e^2} \left(1 - \frac{1}{ikr_e} \right) y,$$

$$H_y = -pk^2 \varepsilon_{\parallel} \sqrt{\varepsilon_{\perp}} \frac{e^{ikr_e}}{r_e^2} \left(1 - \frac{1}{ikr_e} \right) x, \quad (A2)$$

$$H_z = 0.$$

Appendix B: Cartesian presentation of the field of dipole orthogonal to the anisotropy axis

Cartesian components of Eq. (26) for the dipole oriented along y axis, perpendicular to the anisotropy axis z , read:[32]

$$E_x = -pk^2 \frac{\varepsilon_{\parallel}^2}{\sqrt{\varepsilon_{\perp}}} \frac{e^{ikr_e}}{r_e^3} \left(1 - \frac{3}{ikr_e} - \frac{3}{k^2 r_e^2} \right) xy$$

$$- pk^2 \left(\sqrt{\varepsilon_{\perp}} \frac{e^{ikr_o}}{r_o} - \frac{\varepsilon_{\parallel}}{\sqrt{\varepsilon_{\perp}}} \frac{e^{ikr_e}}{r_e} \right) \frac{xy}{x^2 + y^2}$$

$$- ipk \frac{1}{\sqrt{\varepsilon_{\perp}}} (e^{ikr_o} - e^{ikr_e}) \frac{2xy}{(x^2 + y^2)^2}$$

$$E_y = pk^2 \frac{\varepsilon_{\parallel}^2}{\sqrt{\varepsilon_{\perp}}} \frac{e^{ikr_e}}{r_e^3} \quad (B1)$$

$$\times \left[x^2 + \frac{\varepsilon_{\perp}}{\varepsilon_{\parallel}} z^2 - \left(\frac{1}{ikr_e} + \frac{1}{k^2 r_e^2} \right) \left(x^2 + \frac{\varepsilon_{\perp}}{\varepsilon_{\parallel}} z^2 - 2y^2 \right) \right]$$

$$+ pk^2 \left(\sqrt{\varepsilon_{\perp}} \frac{e^{ikr_o}}{r_o} - \frac{\varepsilon_{\parallel}}{\sqrt{\varepsilon_{\perp}}} \frac{e^{ikr_e}}{r_e} \right) \frac{x^2}{x^2 + y^2}$$

$$+ ipk \frac{1}{\sqrt{\varepsilon_{\perp}}} (e^{ikr_o} - e^{ikr_e}) \frac{x^2 - y^2}{(x^2 + y^2)^2},$$

$$E_z = -pk^2 \varepsilon_{\parallel} \sqrt{\varepsilon_{\perp}} \frac{e^{ikr_e}}{r_e^3} \left(1 - \frac{3}{ikr_e} - \frac{3}{k^2 r_e^2} \right) yz,$$

where

$$r_e = \sqrt{\varepsilon_{\parallel}(x^2 + y^2) + \varepsilon_{\perp}z^2},$$

$$r_o = \sqrt{\varepsilon_{\perp}(x^2 + y^2 + z^2)}.$$

Magnetic field reads

$$\begin{aligned} H_x &= -pk^2\varepsilon_{\parallel}\sqrt{\varepsilon_{\perp}}\frac{e^{ikr_e}}{r_e^2}\left(1 - \frac{1}{ikr_e}\right)\frac{y^2z}{x^2 + y^2} \\ &\quad - pk^2\varepsilon_{\perp}\sqrt{\varepsilon_{\perp}}\frac{e^{ikr_o}}{r_o^2}\left(1 - \frac{1}{ikr_o}\right)\frac{x^2z}{x^2 + y^2} \\ &\quad - ipk\sqrt{\varepsilon_{\perp}}\left(\frac{e^{ikr_o}}{r_o} - \frac{e^{ikr_e}}{r_e}\right)\frac{(x^2 - y^2)z}{(x^2 + y^2)^2}, \\ H_y &= pk^2\varepsilon_{\parallel}\sqrt{\varepsilon_{\perp}}\frac{e^{ikr_e}}{r_e^2}\left(1 - \frac{1}{ikr_e}\right)\frac{xyz}{x^2 + y^2} \quad (\text{B2}) \\ &\quad - pk^2\varepsilon_{\perp}\sqrt{\varepsilon_{\perp}}\frac{e^{ikr_o}}{r_o^2}\left(1 - \frac{1}{ikr_o}\right)\frac{xyz}{x^2 + y^2} \\ &\quad - ipk\sqrt{\varepsilon_{\perp}}\left(\frac{e^{ikr_o}}{r_o} - \frac{e^{ikr_e}}{r_e}\right)\frac{2xyz}{(x^2 + y^2)^2}, \\ H_z &= pk^2\varepsilon_{\perp}\sqrt{\varepsilon_{\perp}}\frac{e^{ikr_o}}{r_o^2}\left(1 - \frac{1}{ikr_o}\right)x. \end{aligned}$$

-
- [1] L. B. Felsen and N. Marcuvitz, *Radiation and scattering of waves* (Prentice-Hall Englewood Cliffs, N.J., 1972), ISBN 0137503644.
- [2] D. R. Smith and D. Schurig, Phys. Rev. Lett. **90**, 077405 (2003).
- [3] D. R. Smith, P. Kolinko, and D. Schurig, J. Opt. Soc. Am. B **21**, 1032 (2004).
- [4] W. Cai, U. K. Chettiar, A. V. Kildishev, and V. M. Shalaev, Opt. Express **16**, 5444 (2008).
- [5] H. N. S. Krishnamoorthy, Z. Jacob, E. Narimanov, I. Kretschmar, and V. M. Menon, Science **336**, 205 (2012).
- [6] Z. Jacob and V. M. Shalaev, Science **334**, 463 (2011).
- [7] E. M. Purcell, Phys. Rev. **69**, 681 (1946).
- [8] A. N. Poddubny, P. A. Belov, and Y. S. Kivshar, Phys. Rev. A **84**, 023807 (2011).
- [9] O. Kidwai, S. V. Zhukovsky, and J. E. Sipe, Opt. Lett. **36**, 2530 (2011).
- [10] I. Iorsh, A. Poddubny, A. Orlov, P. Belov, and Y. S. Kivshar, Phys. Lett. A **376**, 185 (2012).
- [11] W. Yan, M. Wubs, and N. Asger Mortensen, ArXiv e-prints (2012), 1204.5413.
- [12] J. Kim, V. P. Drachev, Z. Jacob, G. V. Naik, A. Boltasseva, E. E. Narimanov, and V. M. Shalaev, Opt. Express **20**, 8100 (2012).
- [13] R. K. Fisher and R. W. Gould, Phys. Rev. Lett. **22**, 1093 (1969).
- [14] S. Zhang, Y. Xiong, G. Bartal, X. Yin, and X. Zhang, Phys. Rev. Lett. **106**, 243901 (2011).
- [15] J. Yao, Z. Liu, Y. Liu, Y. Wang, C. Sun, G. Bartal, A. M. Stacy, and X. Zhang, Science **321**, 930 (2008).
- [16] M. A. Noginov, Y. A. Barnakov, G. Zhu, T. Tumkur, H. Li, and E. E. Narimanov, Appl. Phys. Lett. **94**, 151105 (pages 3) (2009).
- [17] L. V. Alekseyev, E. E. Narimanov, T. Tumkur, H. Li, Y. A. Barnakov, and M. A. Noginov, Appl. Phys. Lett. **97**, 131107 (2010).
- [18] C. L. Cortes, W. Newman, S. Molesky, and Z. Jacob, Journal of Optics **14**, 063001 (2012).
- [19] A. A. Orlov, P. M. Voroshilov, P. A. Belov, and Y. S. Kivshar, Phys. Rev. B **84**, 045424 (2011).
- [20] A. V. Chebykin, A. A. Orlov, A. V. Vozianova, S. I. Maslovski, Y. S. Kivshar, and P. A. Belov, Phys. Rev. B **84**, 115438 (2011).
- [21] G. A. Wurtz, W. Dickson, D. O'Connor, R. Atkinson, W. Hendren, P. Evans, R. Pollard, and A. V. Zayats, Opt. Express **16**, 7460 (2008).
- [22] C. R. Simovski, P. A. Belov, A. V. Atrashchenko, and Y. S. Kivshar, Adv. Materials (2012), in press.
- [23] J. Sun, J. Zhou, B. Li, and F. Kang, Appl. Phys. Lett. **98**, 101901 (2011).
- [24] W. Vogel and D.-G. Welsch, *Quantum Optics* (Wiley, Weinheim, 2006).
- [25] P. C. Clemmow, Proc. Inst. Elect. Eng. **110**, 107 (1963).
- [26] H. C. Chen, *Theory of electromagnetic waves: a coordinate-free approach*, McGraw-Hill series in electrical engineering (McGraw-Hill Book Co., 1983).
- [27] W. Weiglhofer, Am. J. Phys. **56**, 1095 (1988).
- [28] W. Weiglhofer, Am. J. Phys. **57**, 455 (1989).
- [29] W. Weiglhofer, IEEE Proc. H **137**, 5 (1990).
- [30] I. V. Lindell, *Methods for electromagnetic field analysis* (Clarendon Press; Oxford University Press, Oxford; New York, 1992).
- [31] P. Cottis, C. Vazouras, and C. Spyrou, IEEE Trans. An-

- tennas Propag. **47**, 195 (1999).
- [32] A. Savchenko and O. Savchenko, *Technical Physics* **50**, 1366 (2005).
- [33] F. P. Sautbekov S., Kanymgazieva I., *Journal of Applied Electromagnetism (JAE)* **10**, **2**, 43 (2008).
- [34] I. M. Gelfand and G. E. Shilov, *Generalized Functions. Volume I: Properties and Operations* (Academic Press, 1964).
- [35] A. Yaghjian, *Proc. IEEE* **68**, 248 (1980), ISSN 0018-9219.
- [36] C. Tai and A. Yaghjian, *Proc. IEEE* **69**, 282 (1981).
- [37] J. Wang, *IEEE Trans. Antennas Propag.* **30**, 463 (1982).
- [38] J. Franklin, *Am. J. Phys.* **78**, 1225 (2010).
- [39] C. P. Frahm, *Am. J. Phys.* **51**, 826 (1983).
- [40] L. Novotny and B. Hecht, *Principles of Nano-Optics* (Cambridge University Press, New York, 2006).
- [41] E. L. Ivchenko, *Optical spectroscopy of semiconductor nanostructures* (Alpha Science International, Harrow, UK, 2005).
- [42] P. C. Clemmow, *Proc. Inst. Elect. Eng.* **110**, 101 (1963).
- [43] I. Lindell, *IEEE Trans. Antennas Propag.* **36**, 1382 (1988).
- [44] I. Lindell, *IEEE Trans. Antennas Propag.* **38**, 353 (1990).